

Improved visible-light activities of nanocrystalline CdS by coupling ultrafine NbN with lattice matching for hydrogen evolution

Yang Qu^a, Ning Sun^a, Muhammad Humayun^a, Amir Zada^a, Ying Xie^a, Junwang Tang^b, Liqiang Jing^{a*} and
Honggang Fu^{a*}

a. Key Laboratory of Functional Inorganic Materials Chemistry (Heilongjiang University), Ministry of Education, School of Chemistry and Materials Science, International Joint Research Center for Catalytic Technology, Harbin 150080, P. R. China. E-mail: jinglq@hlju.edu.cn; fuhg@hlju.edu.cn

b. Department of Chemical Engineering, University College London, Torrington Place, London WC1E 7JE, UK. E-mail: Junwang.tang@ucl.ac.uk

Experimental Section

Synthesis of NbN nanoparticles: Commercial Nb₂O₅ and KOH with molar ratio of 1:20 were well mixed in agitate mortar. The powder sample was transferred into a crucible and annealed at 400 °C for 2 h. The obtained solid was dispersed in hot water and then 1 M HCl was added to it to obtain white precipitate. The precipitate was centrifuged and washed several times with deionized water followed by absolute ethanol and finally dried in vacuum at 60 °C for 4 h. Pure NbN nanoparticles were prepared by annealing the precipitate in NH₃ at 800 °C for 2 h.

Synthesis of NbN/CdS nanocomposites: In a typical synthesis, 30 mg of NbN nanoparticles and a certain amount of cadmium acetate were dispersed in 60 mL of dimethyl formamide (DMF). The suspension was kept in oil bath and heated at 90 °C under vigorous stirring. After that, 10 mL of a certain concentration of sulfourea in DMF solution was dropwise added to it. The resulting mixture was stirred at 90 °C for 1 h and then naturally cooled to room temperature. After that, the obtained product was rinsed three times with deionized water followed by absolute ethanol, and finally dried in vacuum at 60 °C for 4 h. The molar ratio of cobalt acetate and sulfourea was 1:1. The nominal molar ratios of NbN to CdS were R = 0.5, 1, 3 and 5 and the resulting samples were labeled as NC-0.5, NC-1, NC-3 and NC-5, respectively. A pure CdS sample was also prepared for comparison under the same experimental conditions without the addition of NbN. The mechanically mixed NbN/CdS sample was prepared by grinding a certain amount of NbN and CdS in agitate mortar. The sample was named as MNC-R. R = the molar ratios of NbN to CdS.

Photocatalysis:

The photocatalytic H₂ production experiment was conducted in an online photocatalytic H₂ production system (AuLight, Beijing, CEL-SPH2N) at ambient temperature (20±3 °C). In a typical experiment, 100 mg catalyst was suspended in 100 mL of 0.25 M Na₂S and 0.36 M Na₂SO₃ aqueous solution in the reaction cell under magnetic stirring. Prior to the reaction, the mixture was deaerated by evacuation to remove O₂ and CO₂ dissolved in water. The reaction was

carried out by irradiating the mixture with visible-light from a 300 W Xe lamp (AuLight, CEL-HXF300) with a UVCUT filter (AuLight, 400-780 nm). Gas evolution was observed only under photoirradiation, being analyzed by an on-line gas chromatograph (GC-7900, TCD, molecular sieve 5 A, N₂ carrier, Techcomp.).

The determination of the apparent quantum efficiency for hydrogen generation was performed using the same closed circulating system under illumination of a 300 W Xe lamp with bandpass filter ($\lambda=420\text{ nm} \pm 15\text{ nm}$). The light intensity was measured using a Si photodiode (oreal 91105V). The total light intensities was $1.5\text{ mW}\cdot\text{cm}^{-1}$ (420 nm). The irradiation area was around 7 cm^2 . Apparent quantum efficiency (AQE) at different wavelengths was calculated by the following equation.

$$AQE = \frac{2 \times \text{the number of evolved } H_2 \text{ molecules}}{\text{the number of incident photons}} \times 100\%$$

Photoelectrochemical tests:

Photocurrent measurements were performed using a three-electrode configuration, with NC-1, pure CdS, pure NbN and 1wt% Pt/CdS films as the working electrode, saturated Ag/AgCl as the reference electrode, and platinum foil ($3 \times 2\text{ cm}$) as the counter electrode. The working electrode films were prepared by doctor-blade method, using a thin glass rod to roll a paste on FTO to form a film ($2 \times 1\text{ cm}$). The paste was prepared by the dispersion of 0.2 g photocatalyst powder in 0.5 mL ethanol under vigorous stirring for 24 h. The films were annealed at $400\text{ }^\circ\text{C}$ (ramp of $1\text{ }^\circ\text{C min}^{-1}$) for 1 h to make them firm enough. Electrochemical impedance spectroscopy (EIS) measurements were performed in dark and under visible light illumination ($\lambda > 400\text{ nm}$) in 0.5 M Na₂SO₄ solution at open circuit voltage over a frequency range from 10^5 to 0.05 Hz and an AC voltage of 5 mV. The Mott-Schottky plots were obtained at a fixed frequency of 1 kHz in the dark.

Hydroxyl radical measurement:

To detect the amount of hydroxyl radical produced, coumarin fluorescent method was used. In coumarin fluorescent method, 0.02 g powder was dispersed in 50 ml coumarin aqueous solution (0.001 M) in a beaker. Prior to irradiation, the reactor was magnetically stirred for 10 min to attain an adsorption-desorption equilibrium. After irradiation for 1 h with a 150 WGYZ220 high-pressure Xenon lamp (made in China), the sample was centrifuged, and then a certain volume of solution was transferred into a Pyrex glass cell for the fluorescence measurement of 7-hydroxycoumarin at 332 nm excitation wavelength with an emission wavelength of 456 nm through a spectrofluorometer (Perkin-Elmer LS55).

Computational Methods:

Our density functional theory (DFT) calculations employed the linear combination of atomic orbital and spin-unrestricted method implemented in CASTEP code. The generalized gradient approximation (GGA) in Perdew-Burke-Ernzerhof (PBE) functional. The kinetic cut-off energy for the plane-wave basis set was chosen to be 340 eV, the Monkhorst-Pack k-point meshes were set as $5 \times 5 \times 1$, and the ion-electron interactions were modeled by the ultrasoft pseudopotential. The original valence configurations for H, N, O, S, Nb and Cd atoms were 1s1, 2s2 2p3, 2s2 2p4, 3s2 3p4, 4s2 4p6 4d4 5s1 and 4d10 5s2, respectively. To study H₂O adsorption on (002) NbN and (002) Pt with three layers, we employed $2 \times 2 \times 1$ supercell with periodic boundary conditions. The vacuum space was set larger than 15 Å in the z direction to avoid interactions between periodic images. The stable configurations were obtained by geometry optimization from the ideal

unrelaxed structures. The whole optimization procedure was repeated until the average force on the atoms was less than 0.01 eV Å and the energy change less than 1.0×10^{-5} eV/atom.

In order to investigate the H₂O adsorption on adsorbent, we defined the adsorption energy E_{ads} of H₂O molecules on (002) NbN and (002) Pt as follows;

$$E_{\text{ads}} = E_{\text{sur+H}_2\text{O}} - E_{\text{sur}} - E_{\text{H}_2\text{O}}$$

where $E_{\text{sur+H}_2\text{O}}$, E_{sur} and $E_{\text{H}_2\text{O}}$ are the total energy of H₂O molecules on (002) NbN and (002) Pt, isolated surface of (002) NbN and (002) Pt and isolated H₂O.

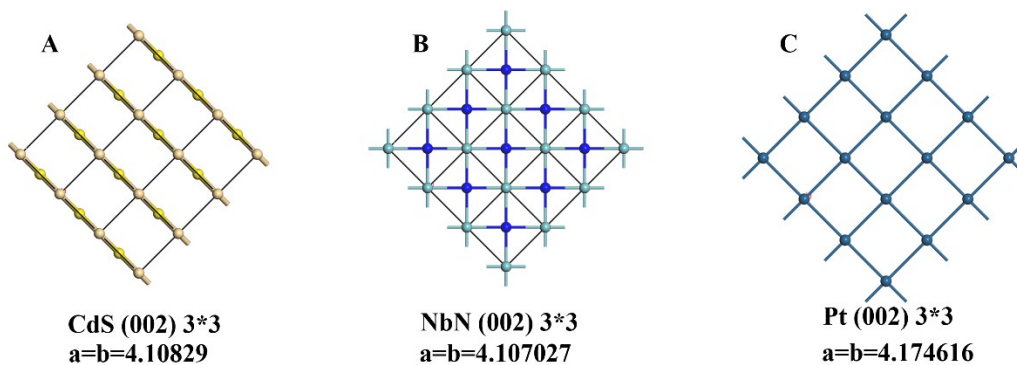


Figure S1. Crystal structure and lattice parameters of (002) CdS, (002) NbN and (002) Pt.

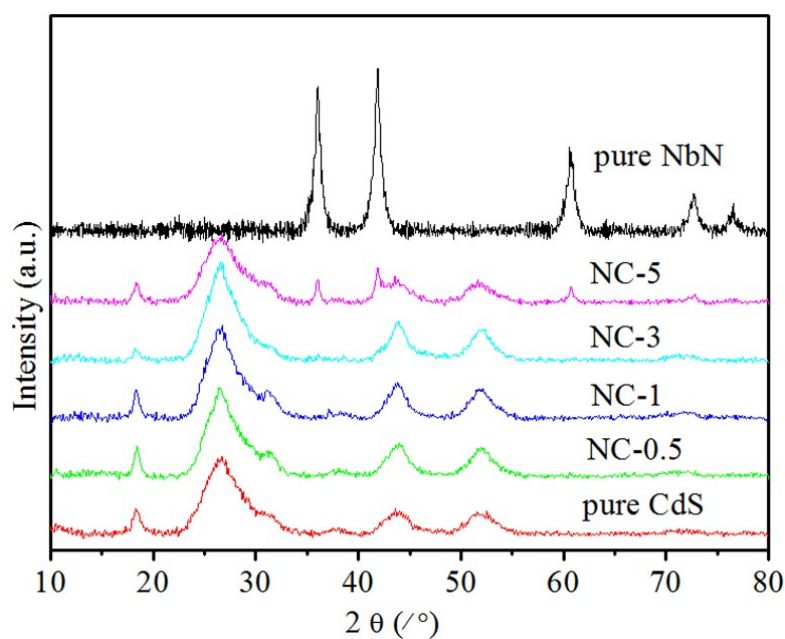


Figure S2 XRD patterns of the bare CdS, NbN and different NbN/CdS nanocomposites.

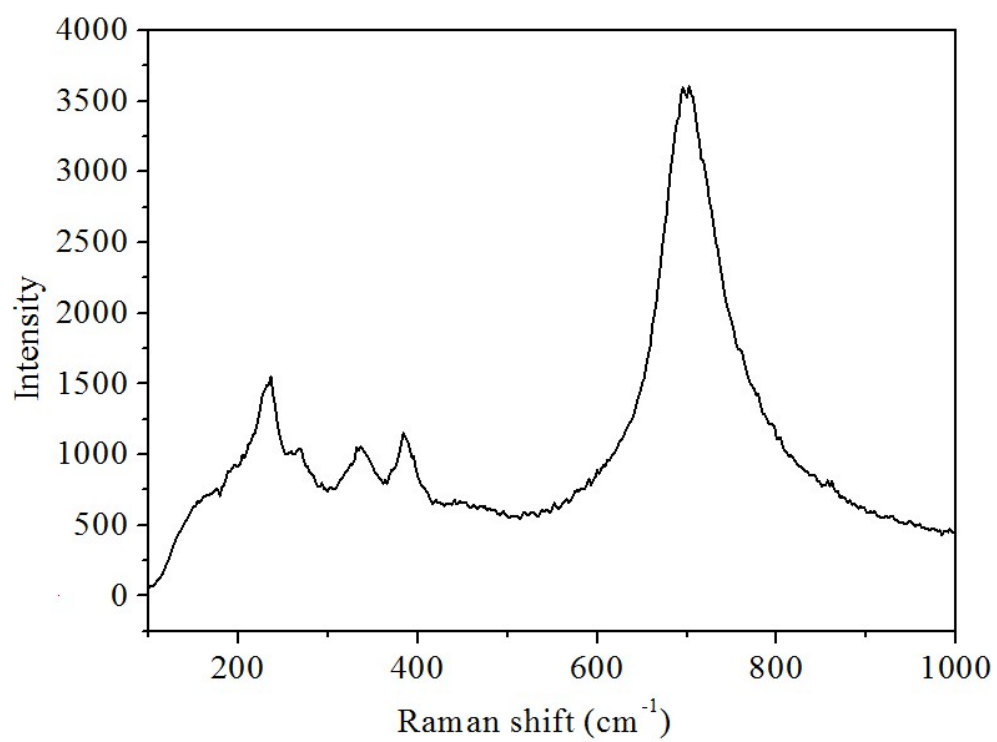


Figure S3 Raman spectrum of pure NbN.

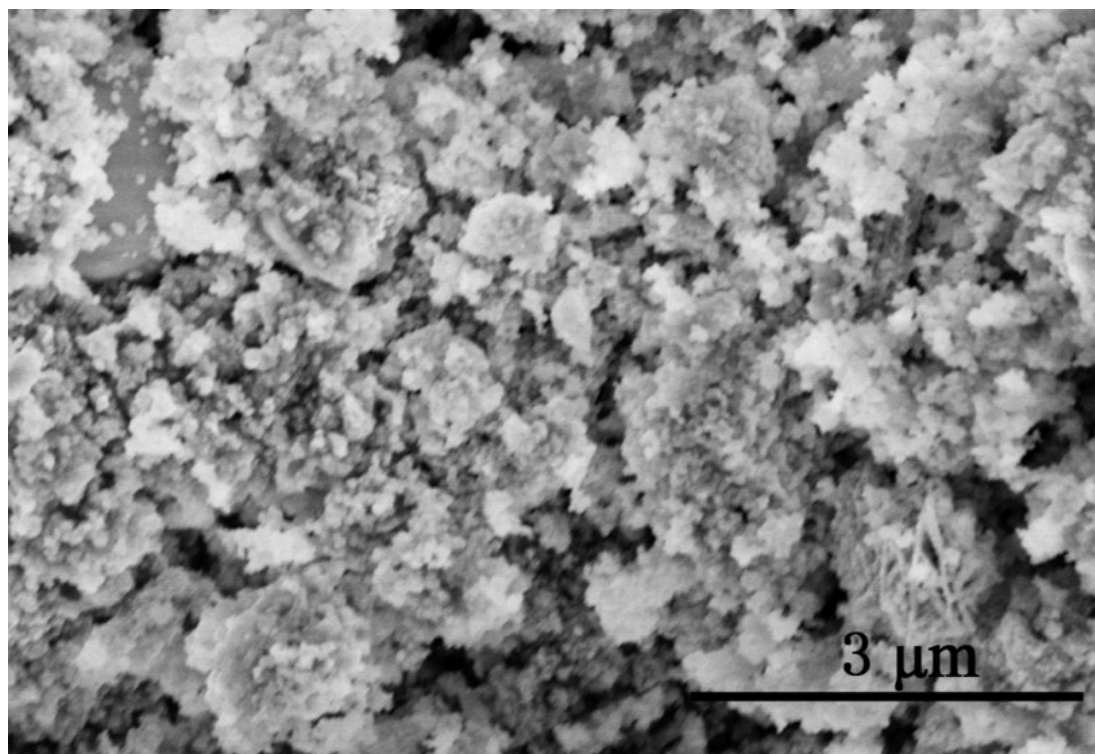


Figure S4 SEM image of pure NbN.

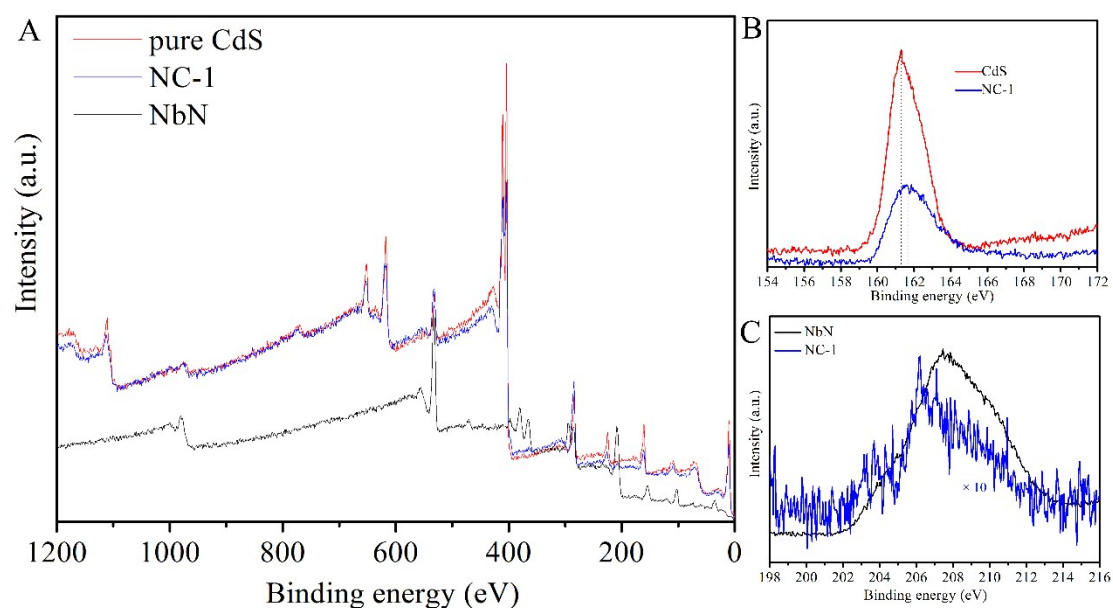


Figure S5 XPS survey spectra of pure NbN, CdS and NC-1 (A), high resolution XPS of S (B) and Nb (C).

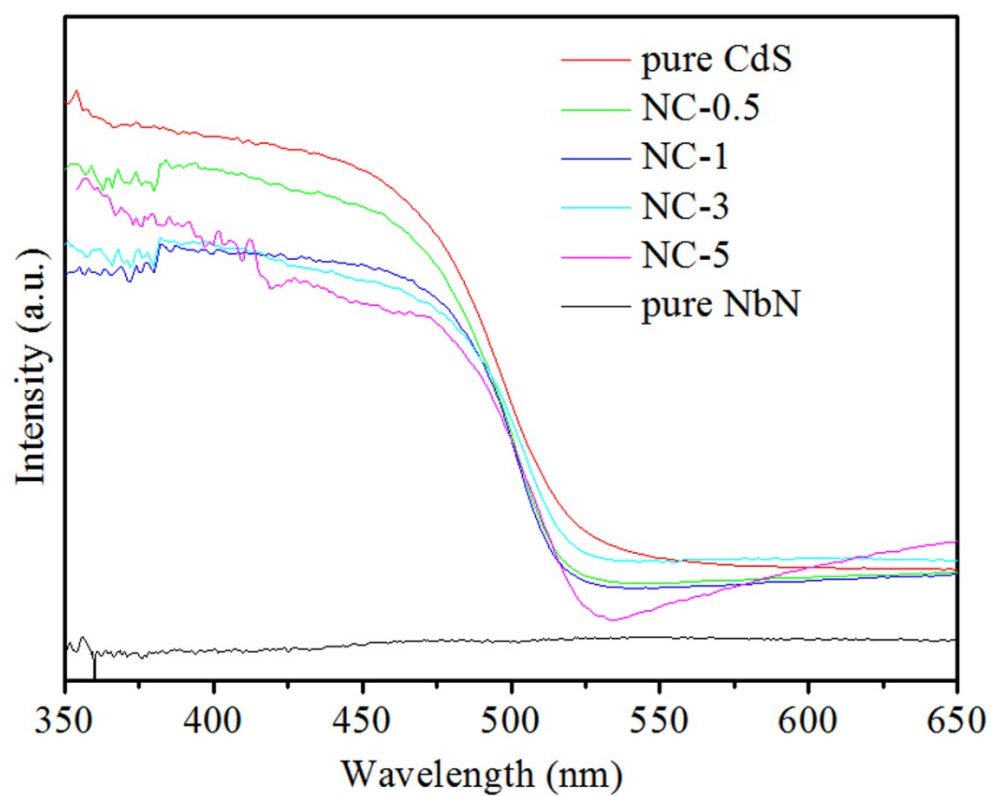


Figure S6 UV-vis absorption spectra of pure CdS, NbN and NbN/CdS nanocomposites.

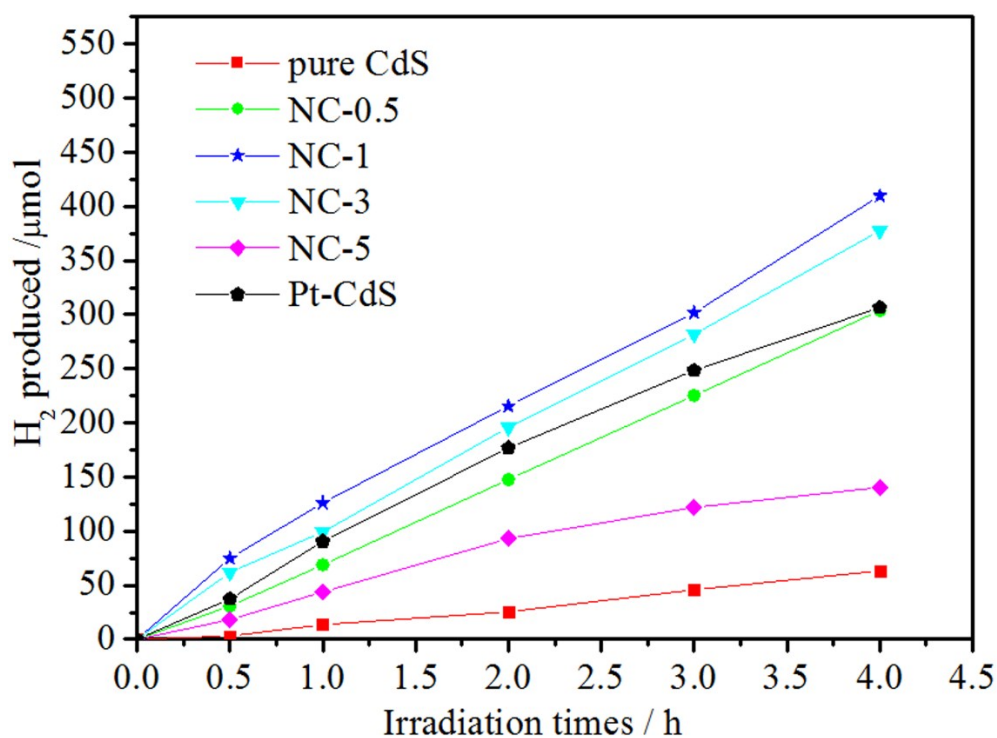


Figure S7 The time course photocatalytic H₂ evolution activity of pure CdS, NbN and NbN/CdS nanocomposites.

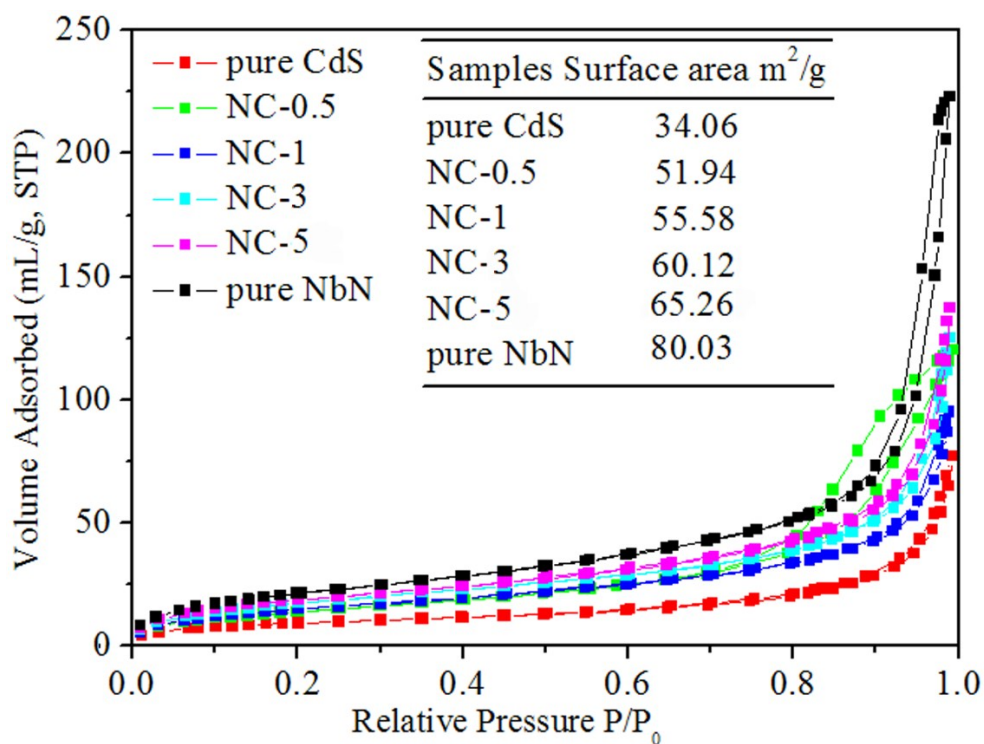


Figure S8 N₂ adsorption-desorption isotherms of pure CdS, NbN and NbN/CdS nanocomposites.

Table S1 Concentration of Cd^{2+} in the solution after visible light irradiation for 12 hours.

Samples	$C_{\text{Cd}^{2+}}$ (ppm)	
	Initial concentration	after irradiation
CdS	1.2	18.4
NC-1	1.4	4.1
Pt/CdS	1.3	11.2

It was measured by atomic absorption spectrometry (AAS, Thermo Elemental SOLAAR-M, limit of identification: $5 \mu\text{g L}^{-1}$). The samples were centrifuged and filtered through $0.22 \mu\text{m}$ nominal pore-size membrane filters prior to analysis.

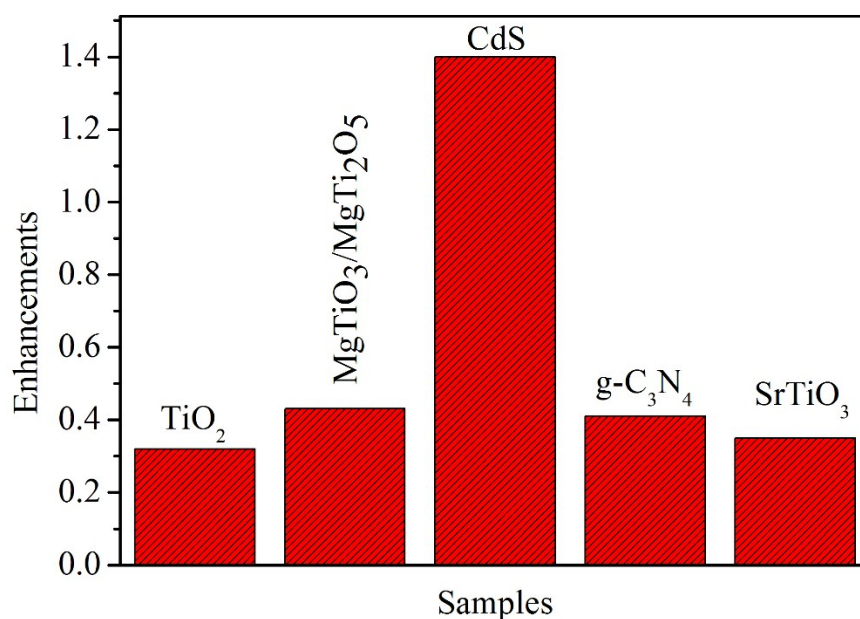


Figure S9 Comparison of the photocatalytic activities enhancement of different semiconductors by loading 1 wt% of NbN nanoparticles. The geometrical lattices of TiO_2 , $\text{MgTiO}_3/\text{MgTi}_2\text{O}_5$ and SrTiO_3 are mismatched to NbN. The photocatalytic hydrogen production experiments are the same as described in experiment section. For the wide bandgap ones of TiO_2 , $\text{MgTiO}_3/\text{MgTi}_2\text{O}_5$ and SrTiO_3 , the light is 300 W Xe lamp with 420 UV cut-off filter. For $\text{g-C}_3\text{N}_4$, the light is visible light which is the same to CdS. The enhancements are calculated as:

$$\text{Enhancement} = \frac{H_2 \text{ amount with NbN}}{H_2 \text{ amount without NbN}}$$

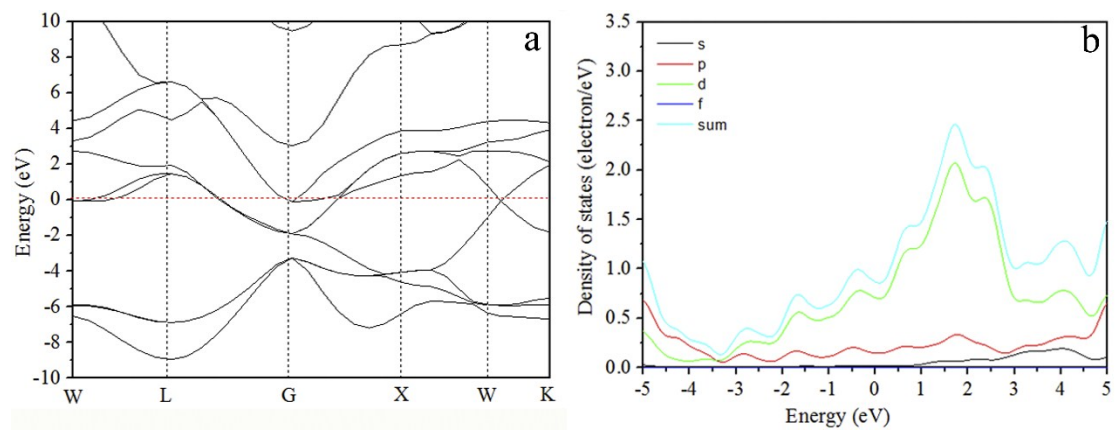


Figure S10 Band diagram (a) and partial density of states (b) of NbN.

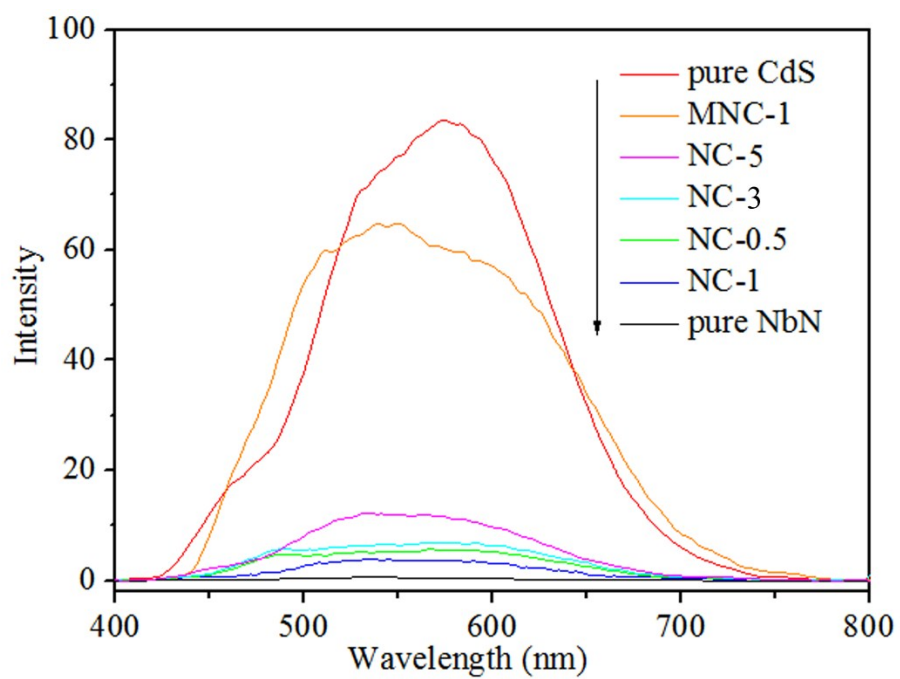


Figure S11 PL spectra of pure CdS, NbN and NbN/CdS nanocomposites.